Electronic Supplementary Information for

Solid state halogen bonded networks vs. dynamic assemblies in solution: explaining N···X interactions of multivalent building blocks

Tiia-Riikka Tero,[a] Kirsi Salorinne,[a] Sami Malola,[b] Hannu Häkkinen[a,b] and Maija Nissinen[a*]

[a] Department of Chemistry, Nanoscience Center, University of Jyvaskyla, P.O. Box 35, FI-40014 Jyvaskyla, Finland

[b] Department of Physics, Nanoscience Center, University of Jyvaskyla, P.O. Box 35 FI-40014 Jyvaskyla, Finland

Contents

1. ^{1}H and ^{13}C NMR Spectra

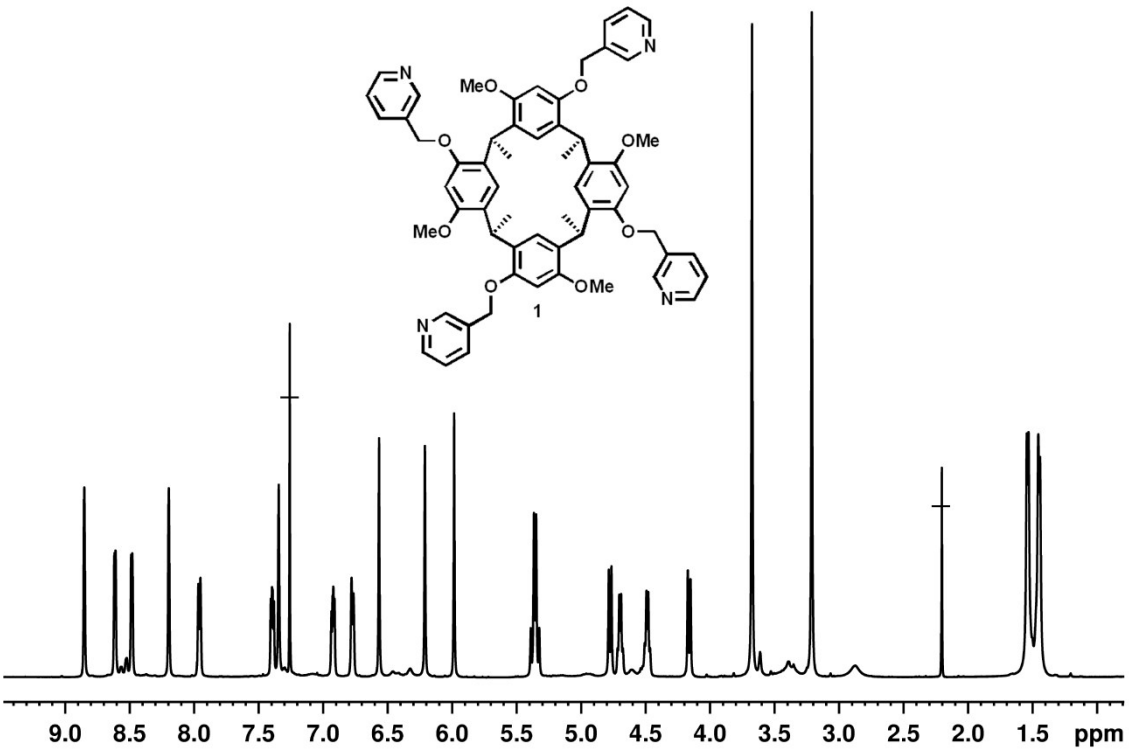

Fig. S1 ^{1}H NMR spectrum of resorcinarene **1** in $CDCl_3$ at -30 °C (500 MHz).

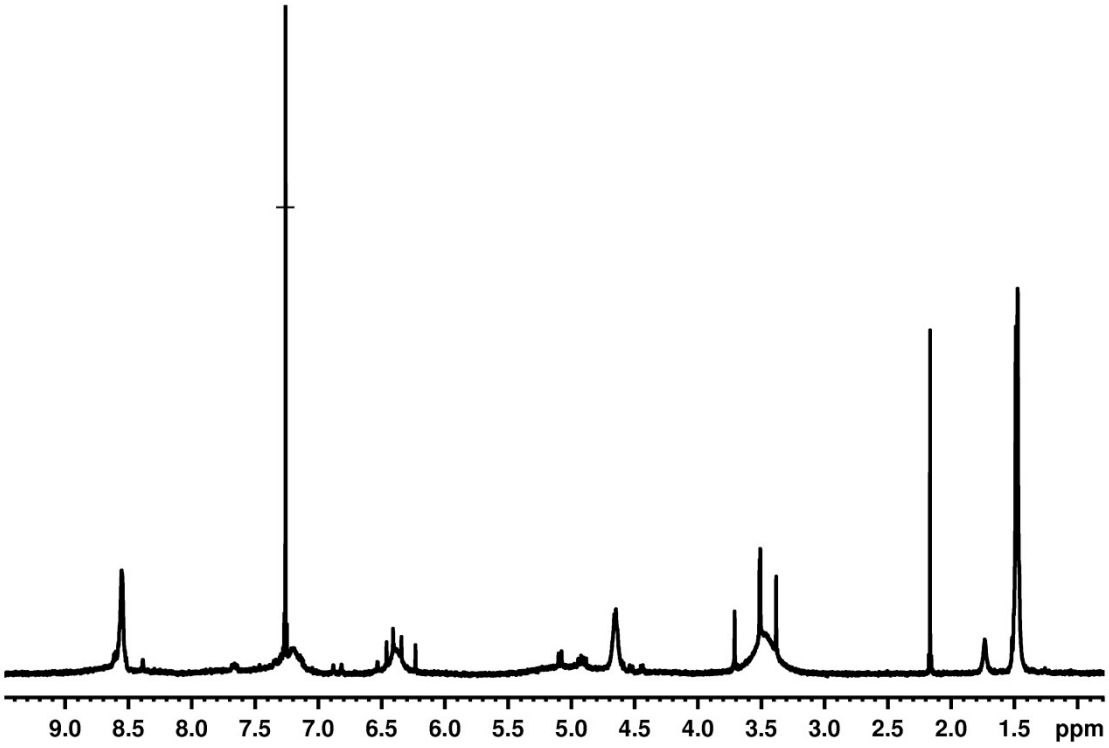

Fig. S2 ^{1}H NMR spectrum of resorcinarene **1** in $CDCl_3$ at 30 °C (500 MHz).

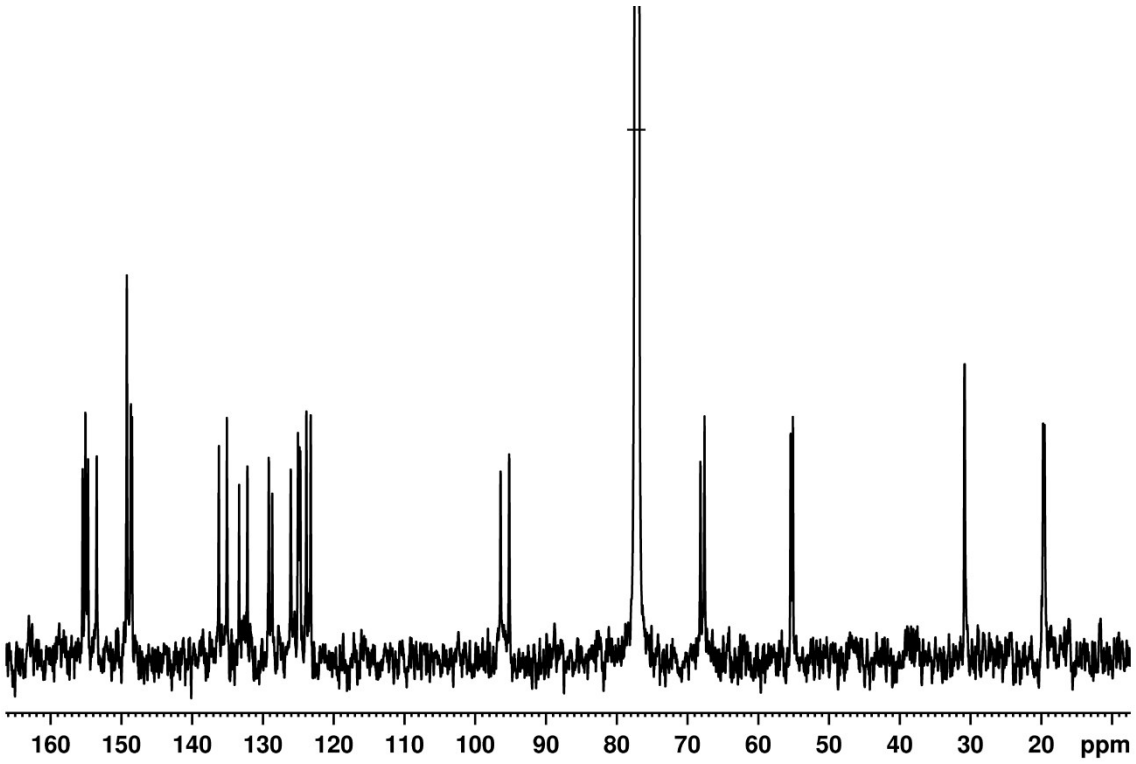

Fig. S3 ^{13}C NMR spectrum of resorcinarene **1** in $CDCl_3$ at -30 °C (126 MHz).

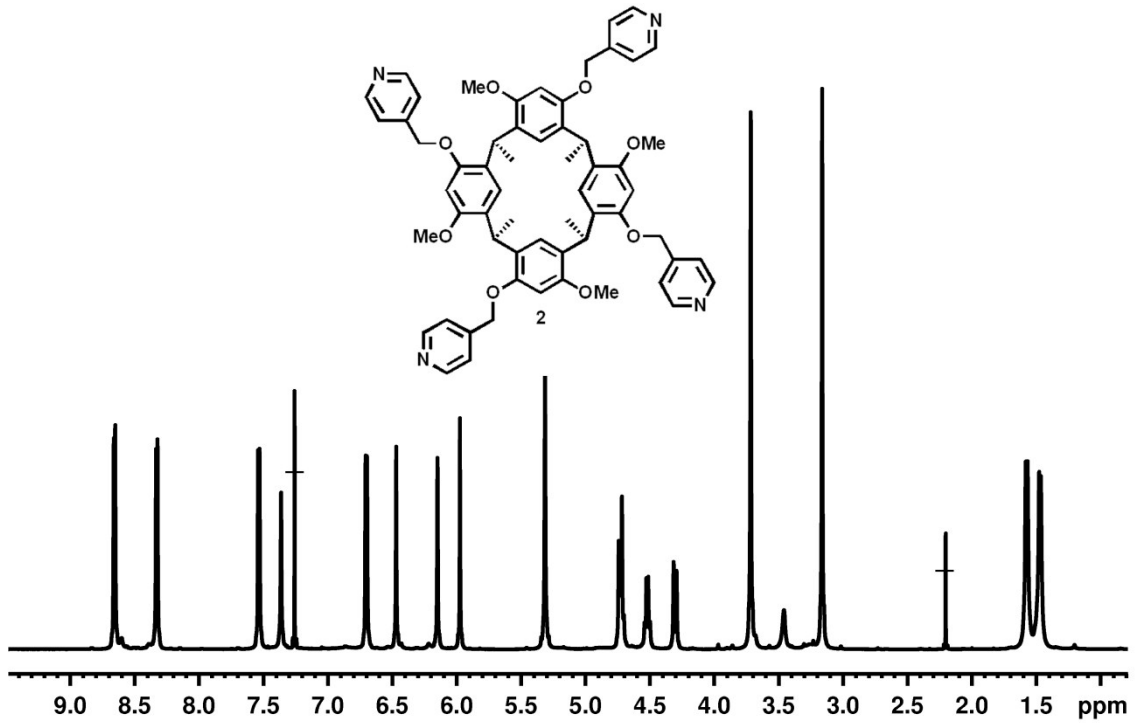

Fig. S4 ^{1}H NMR spectrum of resorcinarene **2** in $CDCl_3$ at -30 °C (500 MHz).

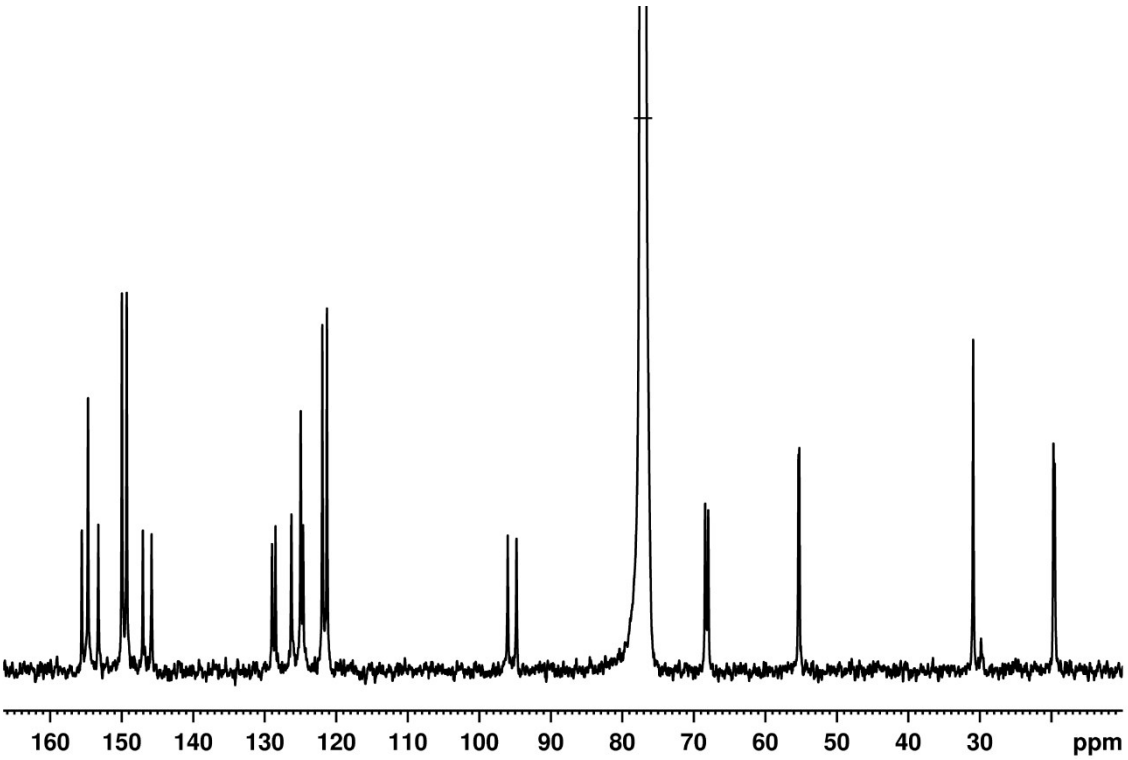

Fig. S5 ^{13}C NMR spectrum of resorcinarene **2** in $CDCl_3$ at -30 °C (126 MHz).

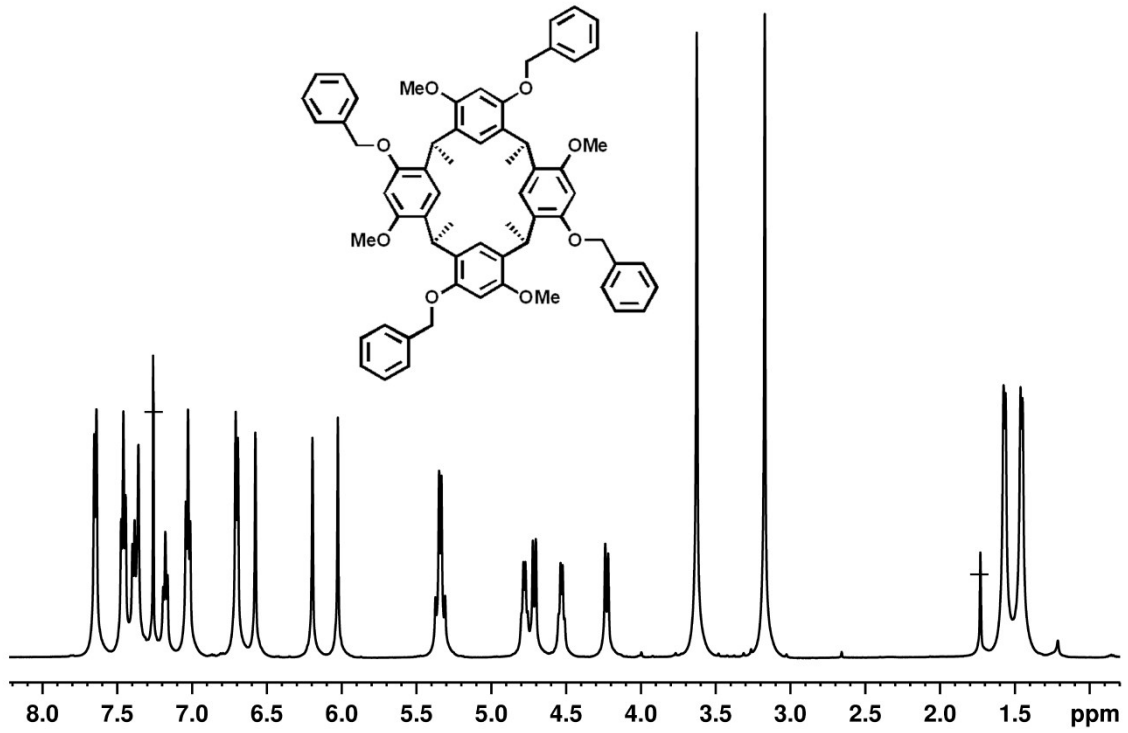

Fig. S6 ^{1}H NMR spectrum of the benzyl functionalized resorcinarene tetrapodand **3** in $CDCl_3$ at -30 °C (500 MHz).

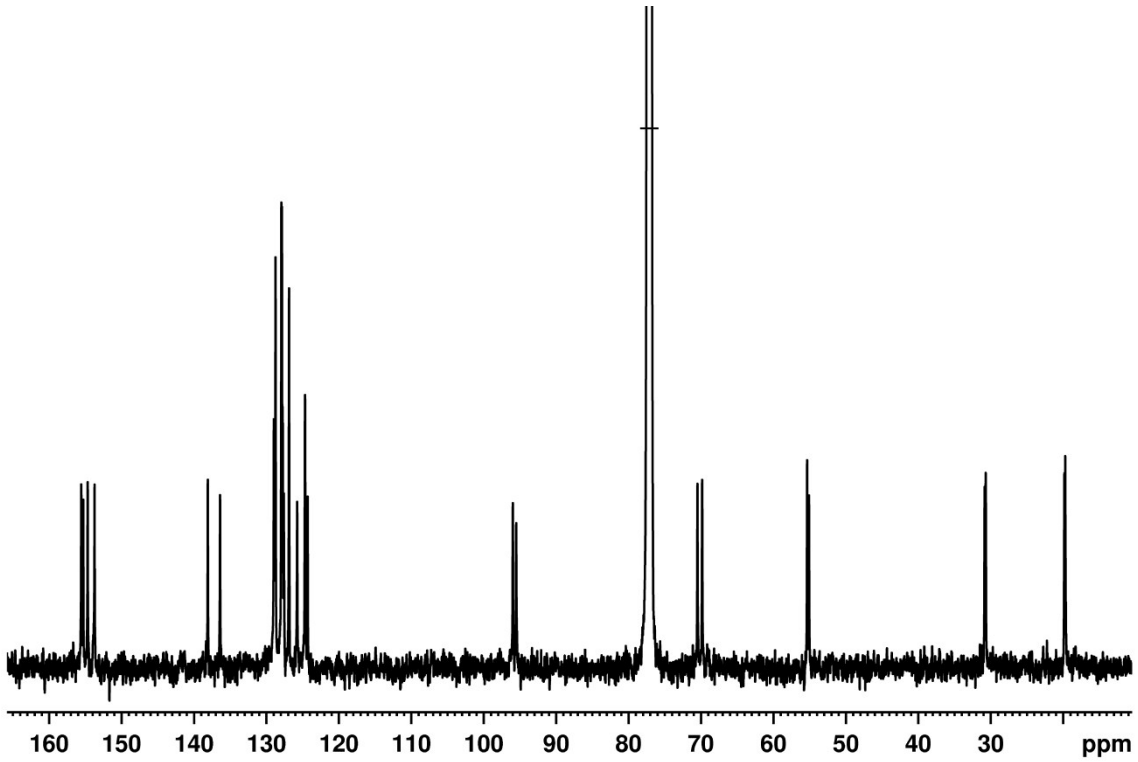

Fig. S7 ^{13}C NMR spectrum of the benzyl functionalized resorcinarene tetrapodand **3** in $CDCl_3$ at -30 °C (126 MHz).

2. Dynamic NMR Measurements

The activation enthalpy and entropy of the interconversions were solved by the method described by Sandström[1] and using the rate constants obtained from line shape analyses and Eyring equation. Lineshape calculations for measured ^1H NMR spectra at different temperatures where performed using Bruker TopSpin 3.2 DNMR Lineshape Analysis module. Methine proton (CH) and CH_2 of the pyridine arm of the resorcinarenes **1** and **2** were included into the mutually exchanging spin system model for the lineshape analysis (4.30-4.85 ppm for **1** and 4.40-4.85 ppm for **2**). The activation enthalpy and entropy of **1** and **2** were determined using the equation (1).

$$\log(k/T) = 10.32 - \Delta H^{\ddagger}/19.14T + \Delta S^{\ddagger}/19.14, \quad (1)$$

where k (s^{-1}) is a rate constant obtained from spectral fitting, T is temperature (K), $\Delta H^{\ddagger}$ in $kJmol^{-1}K^{-1}$ and $\Delta S^{\ddagger}$ in $Jmol^{-1}K^{-1}$. Thus, the plot $\log(k/T)$ against $1/T$ affords a slope of "$-\Delta H^{\ddagger}/19.14$" and an intercept at $1/T=0$ of "$\Delta S^{\ddagger}/19.14+10.32$".

[1] J. Sandström in *Dynamic NMR Spectroscopy*; Academic Press Inc.: London, United Kingdom, **1982**.

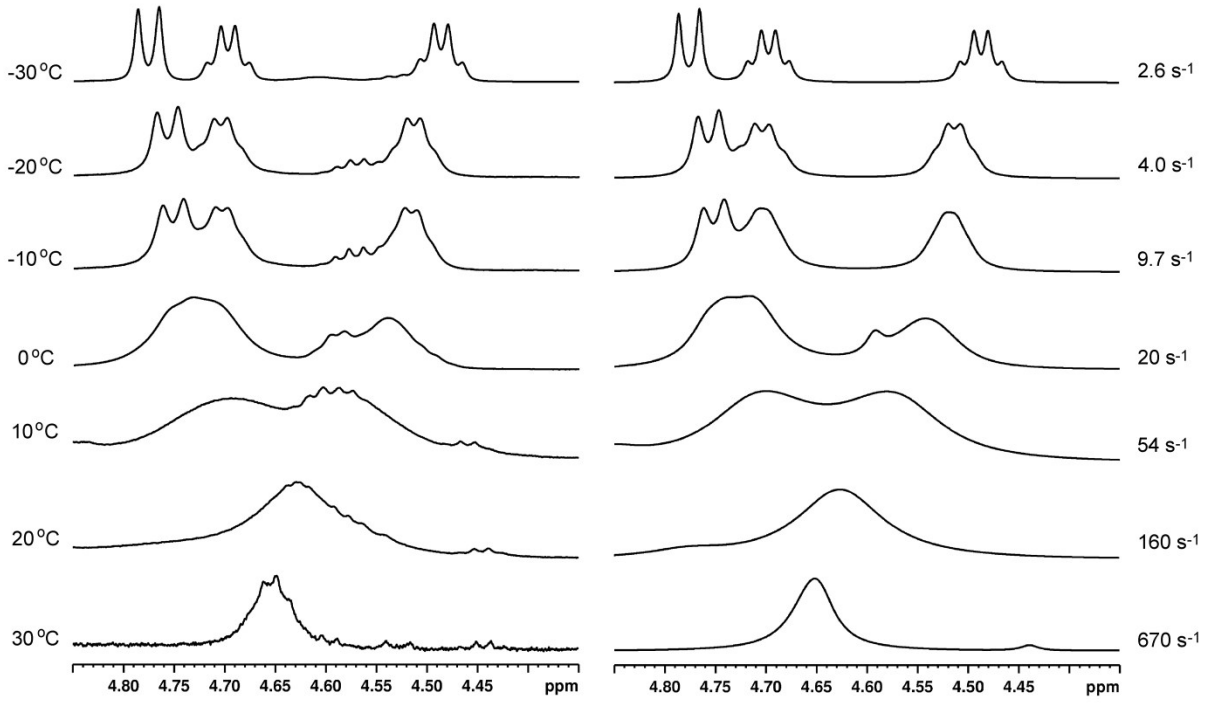

Fig. S8 Experimental (left) and fitted (right) ^{1}H NMR spectra of resorcinarene **1** at different temperatures.

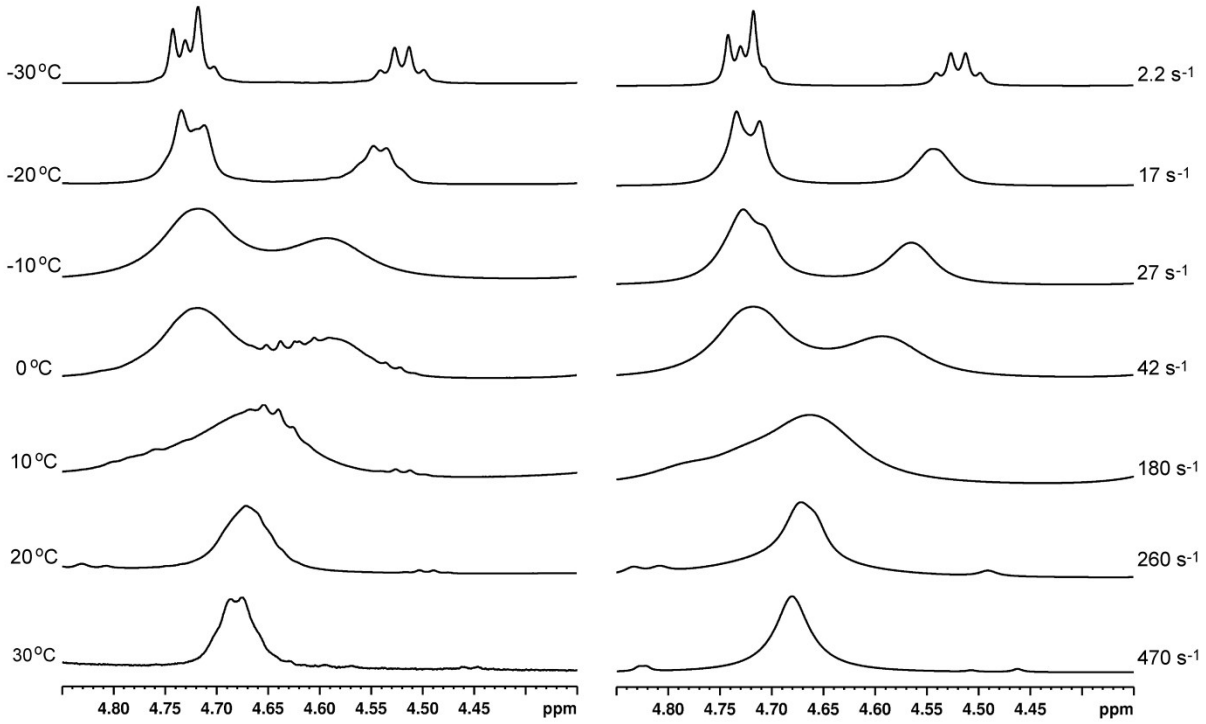

Fig. S9 Experimental (left) and fitted (right) ^{1}H NMR spectra of resorcinarene **2** at different temperatures.

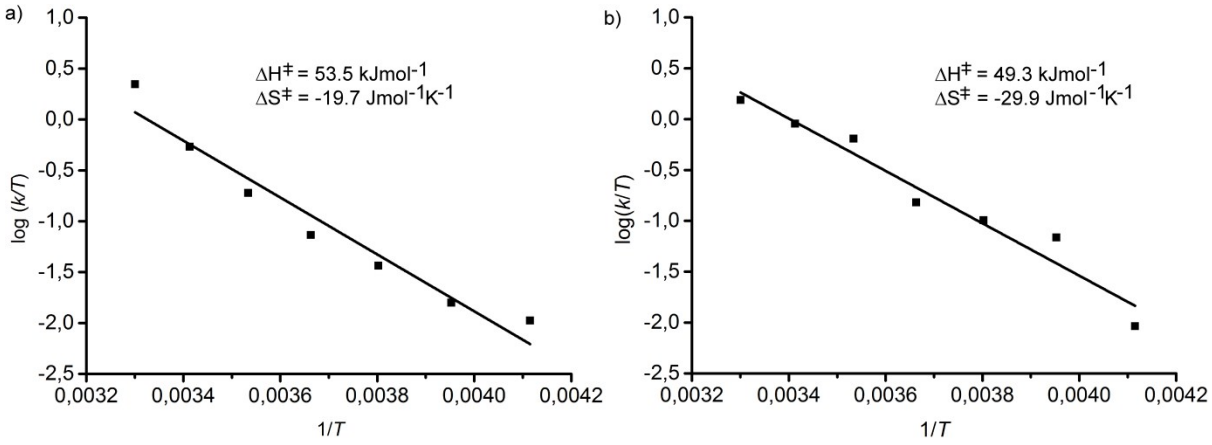

Fig. S10 Eyring plot and activation enthalpy and entropy from the calculated rate constants for the *boat*$_1$-*boat*$_2$ interconversion of the resorcinarene derivatives **1** (a) and **2** (b).

3. Crystal Structure Determination

Structure 2-MeCN ($C_{60}H_{60}N_4O_8 \cdot CHCl_3 \cdot 2$ MeCN): Colorless block crystals (0.08 x 0.18 x 0.20 mm) were crown from acetonitrile-chloroform solution of **2** with slow evaporation at 2-8 °C. A nitrogen of one of the acetonitrile molecules is disordered over two positions (N22A and N22B, 0.5:0.5). The absorption correction was not used.

Structure 2-CHCl$_3$ ($C_{60}H_{60}N_4O_8 \cdot 3\ CDCl_3$): Colorless, fragile plate crystals (0.17 x 0.24 x 0.35 mm) were obtained from an NMR sample of 1:1 ratio of **2** and 1,4-dibromotetrafluorobenzene in $CDCl_3$ with slow evaporation at 2-8 °C. Chlorine atoms of one of the chloroform molecules are disordered over three positions (CL4, CL5 and CL6, 0.3:0.4:0.3) and the bond distances of C201-CL4C and C201-CL5C are restrained to be 1.79 Å (DFIX). This chloroform molecule was refined isotropically. A chlorine atom of another chloroform molecule is disordered over two positions (CL7A and CL7B, 0.5:0.5) and the temperature factor of CL7A is equalized with the temperature factor CL7B (EADP). The bond between C301 and CL7B is restrained to be 1.79 Å (DFIX).

Structure 1-MeOH ($C_{60}H_{60}N_4O_8 \cdot 3\ CH_3OH$): Colorless block crystals (0.11 x 0.13 x 0.28 mm) were crown from methanol-chloroform solution of **1** with slow evaporation at room temperature within few days.

Structure 2-EtOH ($C_{60}H_{60}N_4O_8 \cdot CHCl_3 \cdot\ CH_3CH_2OH$): Colorless block crystals (0.10 x 0.14 x 0.20 mm) were crown from ethanol-chloroform solution of **2** with slow evaporation at 2-8 °C. A carbon of the solvent ethanol is disordered over two positions (C20A and C20B 0.5:0.5. The temperature factor of C20A is equalized with the temperature factor C20B (EADP) and the bonds between carbons C201-C20A and C201-C20B are restrained to be 1.54 Å (DFIX), and the bond between C201-O200 to 1.43 Å (DFIX). A reasonable disorder

model could not be constructed for the chloroform because of the lack of electron density. The absorption correction was not used.

Structure 1-B ($C_{60}H_{60}N_4O_8 \cdot 1.5\ C_6F_4I_2 \cdot CDCl_3$): Colorless plate crystals (0.03 x 0.13 x 0.15 mm) were obtained from an NMR sample of 1:1 ratio of **1** and 1,4-diiodotetrafluorobenzene in $CDCl_3$ with slow evaporation at 2-8 °C. The crystals were significantly stronger than the fragile crystals without a halogen linker. Residual electron density suggested that the unit cell includes a highly disordered chloroform molecule in addition to the found, ordered chloroform solvent. No reasonable model for the disordered molecule could be built and the SQUEEZE option in PLATON[2] was used to remove the electron density. The size of the remaining void shows that the solvent included in the position has enough space to obtain several different positions leading to severe disorder.

Structure 2-B ($0.5\ C_{60}H_{60}N_4O_8 \cdot C_6F_4I_2 \cdot CHCl_3$): 1,4-diiodotetrafluorobenzene (2 eq) in methanol was slowly added on top of **2** (1 eq) in chloroform. With slow evaporation at 2-8 °C colorless needle-like, strong crystals (0.03 x 0.13 x 0.15 mm) were obtained.

Table S1. Conformational properties of the resorcinarene core and podand arms in the crystal structures.

	2-MeCN	**2**-$CHCl_3$	**1**-MeOH	**2**-EtOH	**1-B**	**2-B**
Dihedral angle[a] (°)	81.4/89.6 171.8/173.3	83.0/84.5 186.2/183.9	82.5/83.7 175.8/187.7	80.1/88.2 186.9/178.1	85.1/81.3 182.9/188.9	83.6/83.6 189.3/189.3
Angle[b] (°)	-8.2/165.1	-12.7/190.1	-14.1/185.2	-10.9/165.1	-14.00/191.2	-12.7/198.5
Tilt (°)	4.6	3.8	4.0	0.4	4.6	17.8
Twist (°)	4.2	3.5	5.8	0.5	4.9	17.5
Pyridine arm torsion[c] (°)	-170.5/168.5/ -168.6/-69.6	178.9/-168.7/ 171.8/72.9	-160.6/-179.9/ -171.4/-173.4	-171.7/172.2/ -164.4/177.2	-168.1/170.6/ -158.0/-179.1	-172.9/-171.8/ -172.9/-171.8
	Type II	Type II	Type I	Type I	Type I	Type I

[a]Dihedral angles between the methine plane (C7-C14-C21-C28) and the vertical and the horizontal aromatic rings. [b]Between the opposite aromatic ring planes. [c]Torsion of Ar**C**-**O**-**C**H_2-Py**C**.

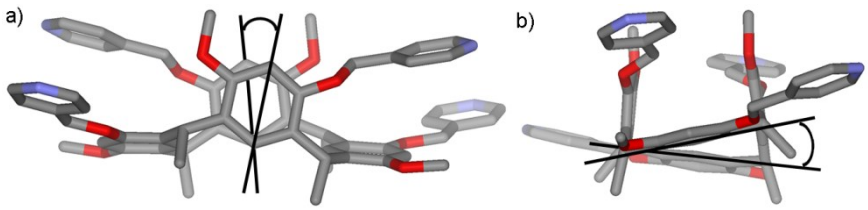

Fig. S11 a) Tilt and b) twist angles of resorcinarene derivatives **1**-**2** (shown for structure **2**-**B**). Hydrogen atoms have been omitted for clarity.

[2] PLATON 1980-2009 v. 260109

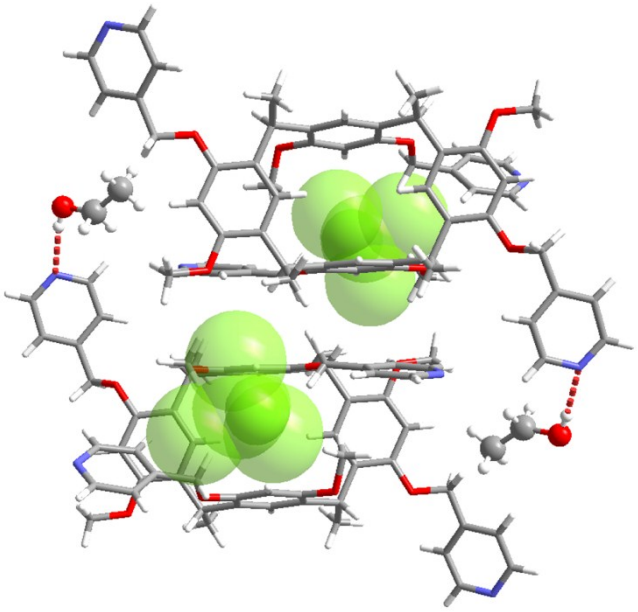

Fig. S12 Ethanol molecule forming a hydrogen bond (2.23 Å) with one of the pyridine rings of the resorcinarene **2** in the structure **2**-EtOH. Chloroform molecules (space fill model) are located on top of the macrocycle cavities. Resorcinarene enantiomers of different inherent chirality are packed next to each other their cavities pointing to opposite direction. Hydrogen bonds are shown as red dash lines.

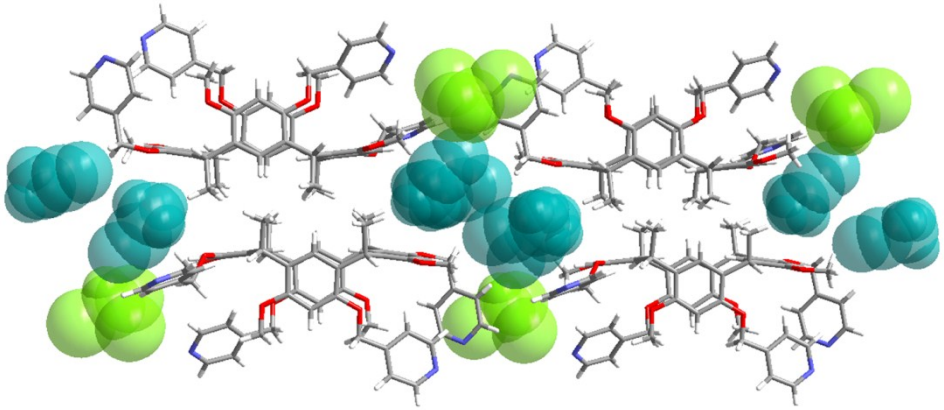

Fig. S13 Crystal packing in the structure **2**-MeCN showing how chloroform and acetonitrile molecules (space fill model) fill the voids between resorcinarene stacks. Chloroform molecules are shown in light green and acetonitrile molecules in turquoise.

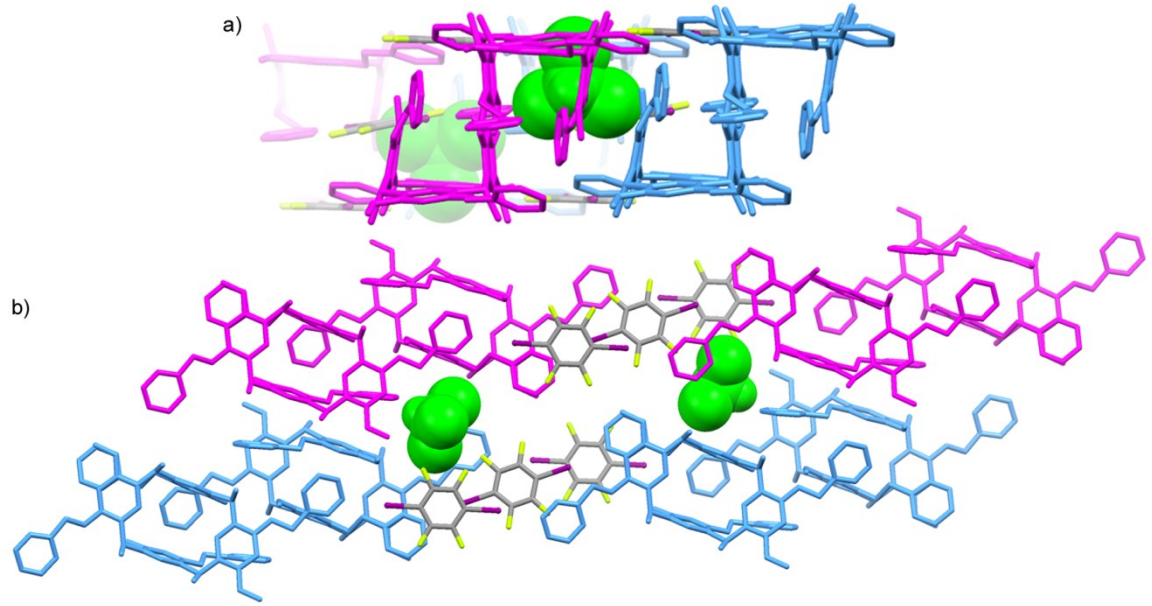

Fig. S14 Side (a) and top (b) view of packing of double chains horizontally in structure **1-B**. The linkers are shown in elemental colors and the resorcinarenes of the same double chain in blue and in magenta. Chloroform molecules are shown as a space fill model in green. Hydrogen atoms have been omitted for clarity.

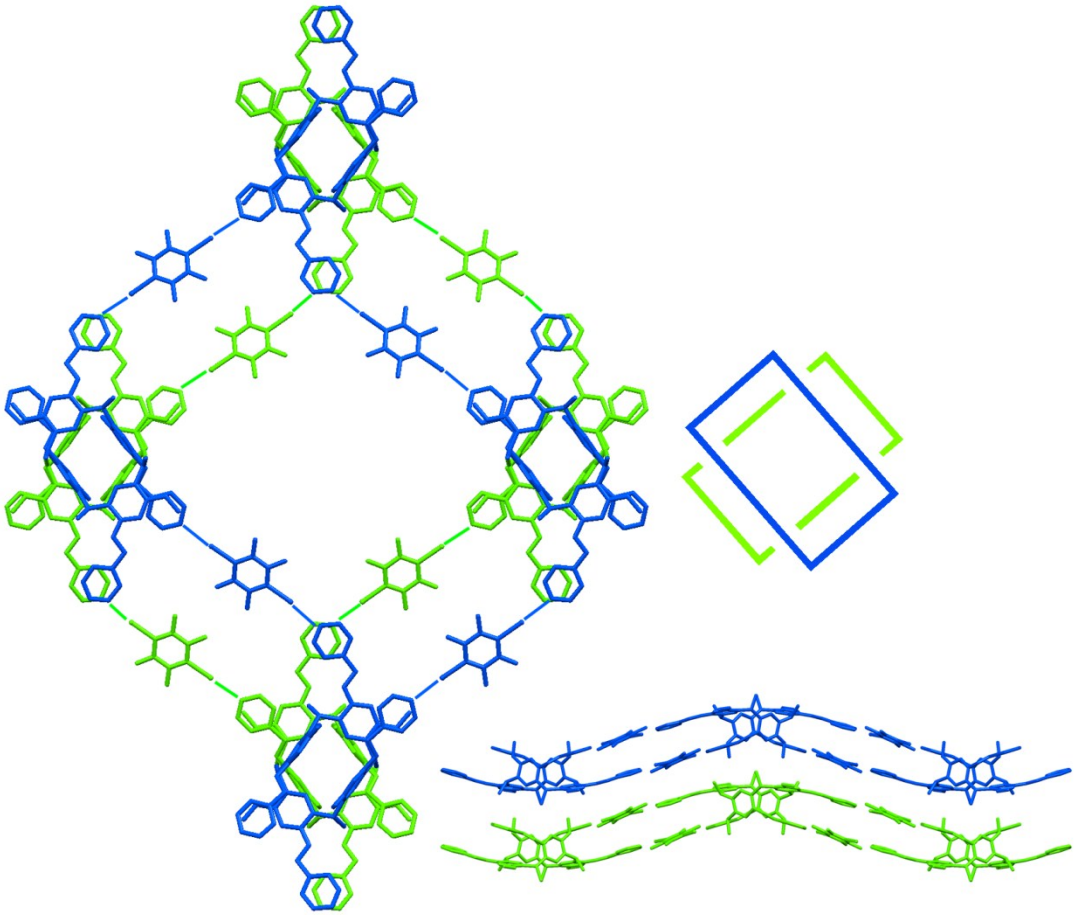

Fig. S15 Top and side views of the stacked grids of resorcinarenes with different inherent chirality in structure **2**-**B**. Hydrogen atoms have been omitted for clarity. Schematic presentation on the right shows the antiparallel arrangement of layers.

4. Analyses of Halogen Bonds in Solution

KF (-125.3 ppm) was used as the inner standard in ^{19}F NMR measurements.

^{19}F NMR measurements

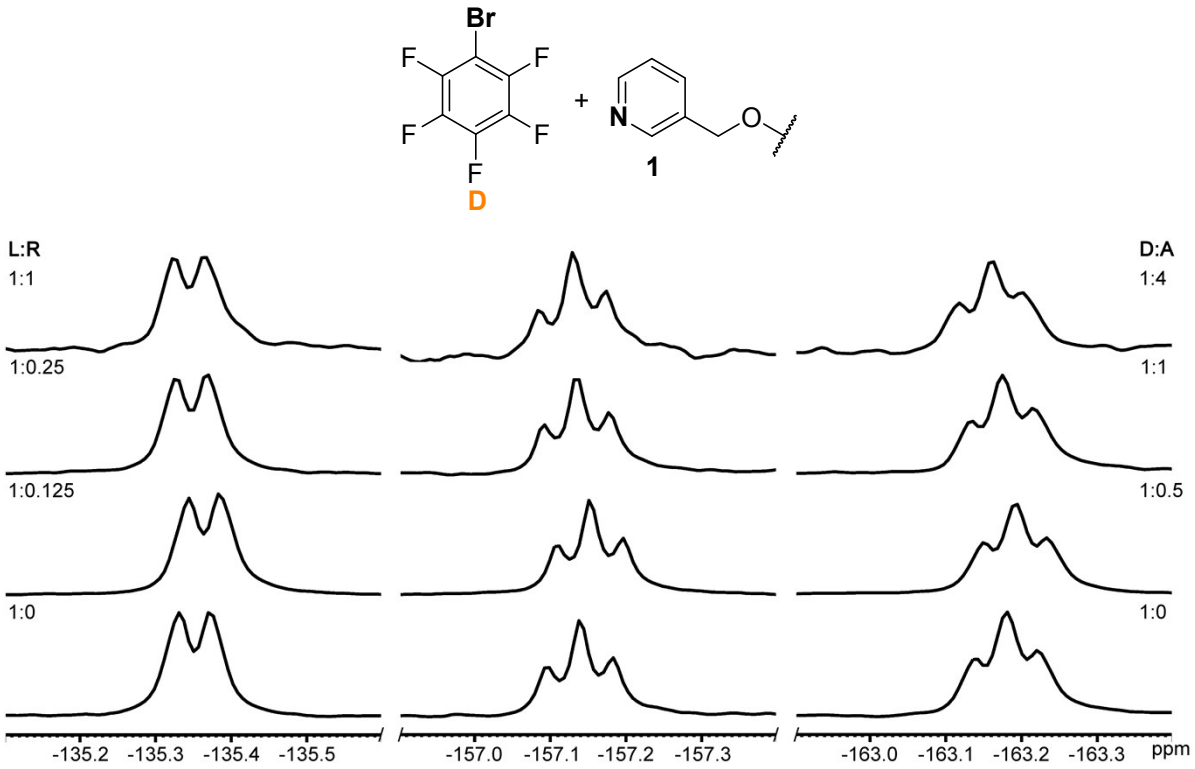

Fig. S16 ^{19}F NMR spectra of linker **D** with resorcinarene **1** at 30°C (280 MHz) showing the fluorine chemical shift changes at different linker:resorcinarene (L:R) concentrations. Halogen bond donor:acceptor (D:A) ratios are shown right.

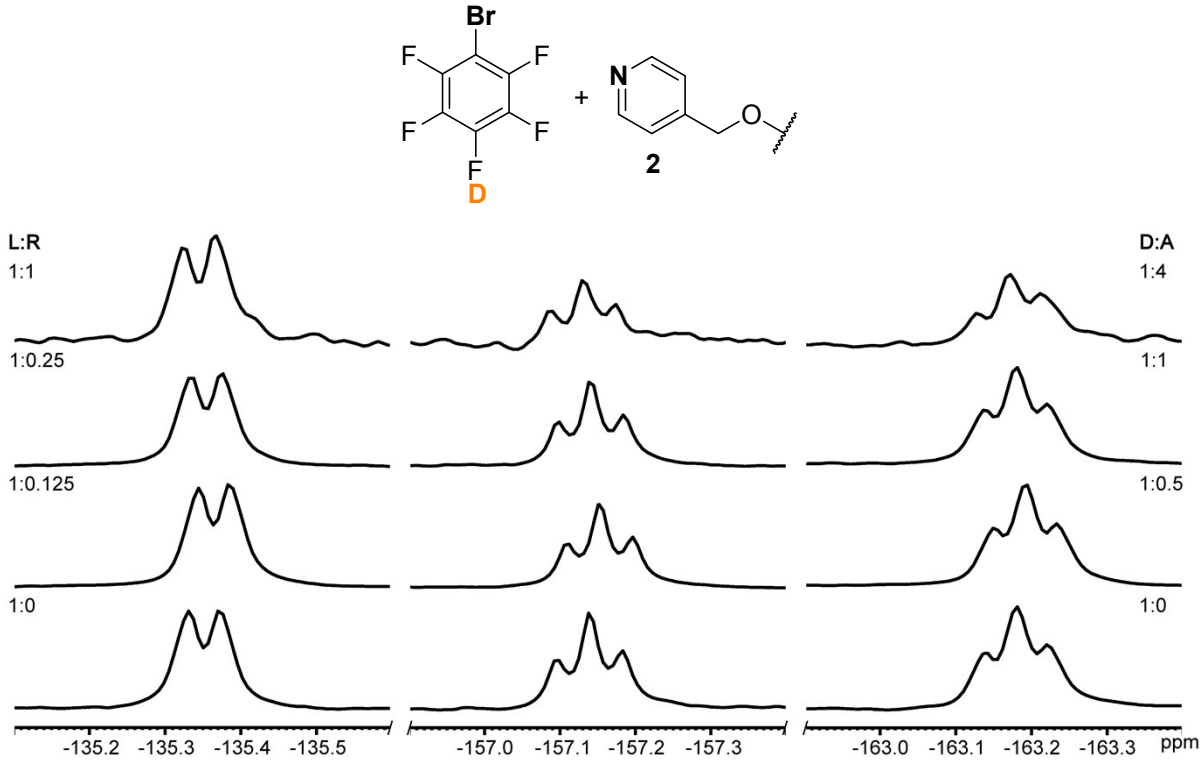

Fig. S17 ^{19}F NMR spectra of linker **D** with resorcinarene **2** at 30°C (280 MHz) showing the fluorine chemical shift changes at different linker:resorcinarene (L:R) concentrations. Halogen bond donor:acceptor (D:A) ratios are shown right.

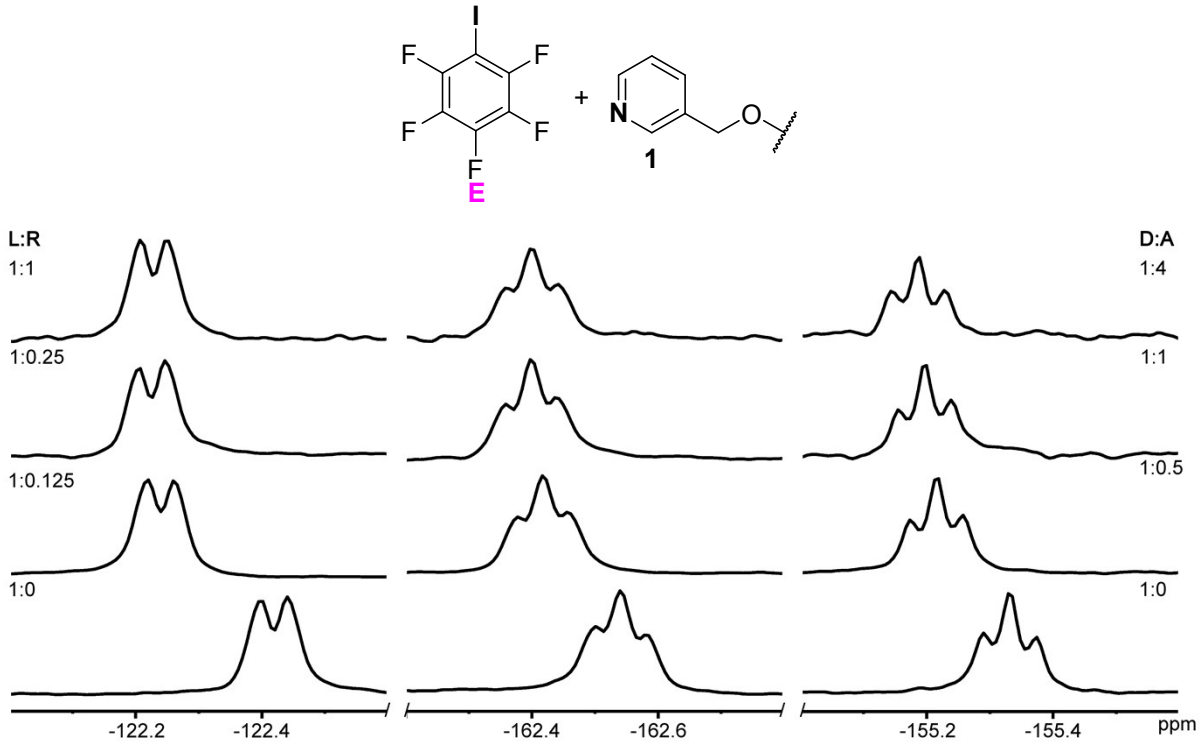

Fig. S18 ^{19}F NMR spectra of linker **E** with resorcinarene **1** at 30°C (280 MHz) showing the fluorine chemical shift changes at different linker:resorcinarene (L:R) concentrations. Halogen bond donor:acceptor (D:A) ratios are shown right.

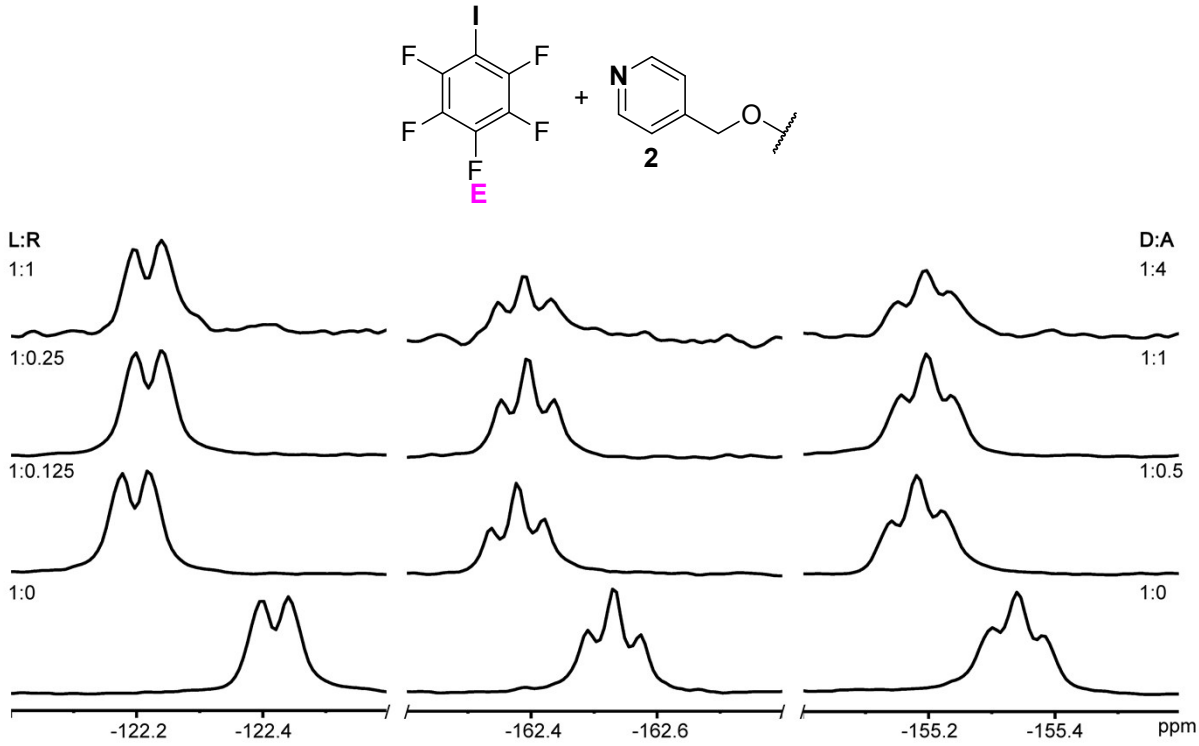

Fig. S19 ^{19}F NMR spectra of linker **E** with resorcinarene **2** at 30°C (280 MHz) showing the fluorine chemical shift changes at different linker:resorcinarene (L:R) concentrations. Halogen bond donor:acceptor (D:A) ratios are shown right.

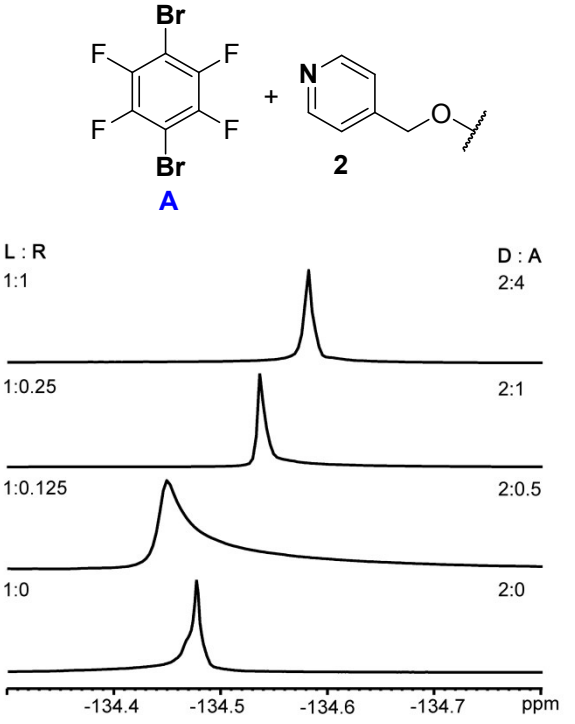

Fig. S20 ^{19}F NMR spectra of linker **A** with resorcinarene **2** at 30°C (280 MHz) showing the fluorine chemical shift changes at different linker:resorcinarene (L:R) concentrations. Halogen bond donor:acceptor (D:A) ratios are shown right.

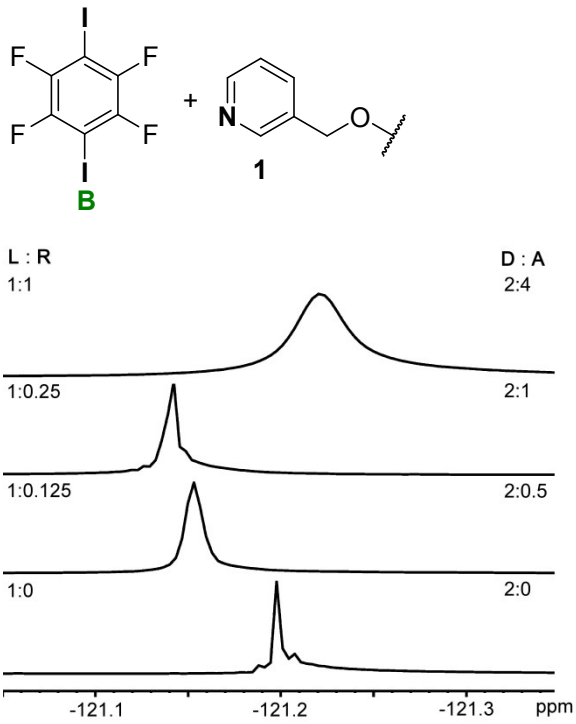

Fig. S21 ^{19}F NMR spectra of linker **B** with resorcinarene **1** at 30°C (280 MHz) showing the fluorine chemical shift changes at different linker:resorcinarene (L:R) concentrations. Halogen bond donor:acceptor (D:A) ratios are shown right.

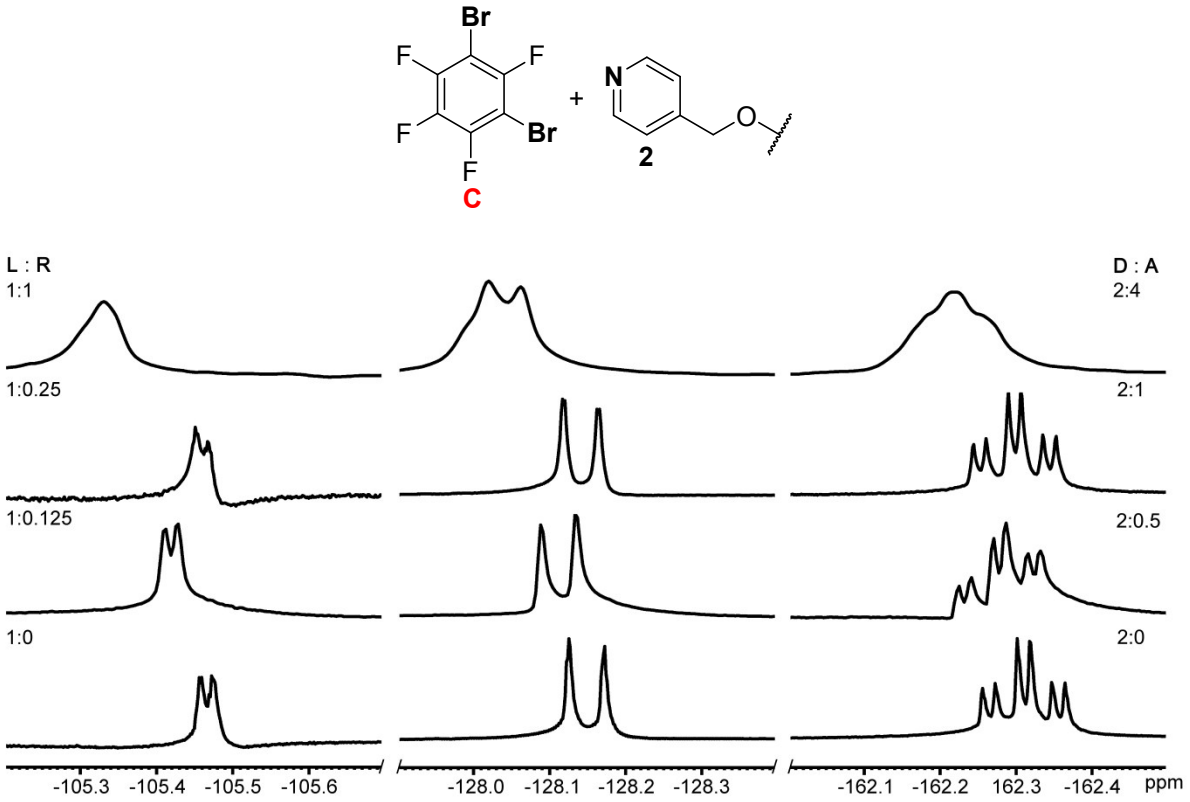

Fig. S22 ^{19}F NMR spectra of linker **C** with resorcinarene **2** at 30°C (280 MHz) showing the fluorine chemical shift changes at different linker:resorcinarene (L:R) concentrations. Halogen bond donor:acceptor (D:A) ratios are shown right.

^{1}H NMR measurements

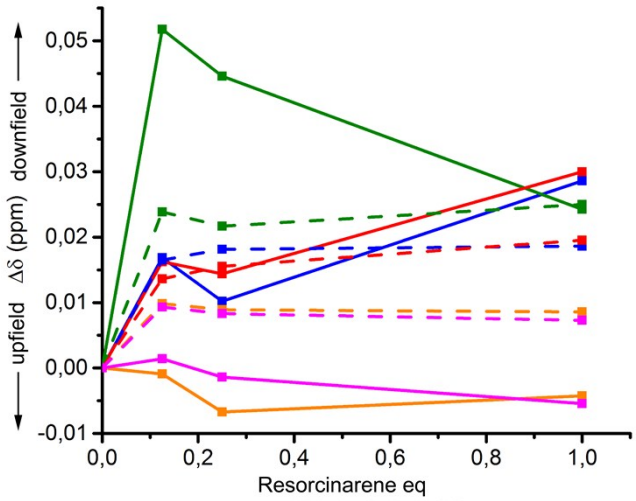

Fig. S23 ^{1}H NMR signal shifts (ppm) of pyridine protons of linker **A**-**E** (blue, green, red, orange, magenta) mixtures with increasing amounts of resorcinarenes **1** (solid line) and **2** (dash line). The shifts are averaged from the two pyridine ring signals that were affected by addition of linkers.

Diffusion ordered NMR

Diffusion ordered NMR spectroscopy (DOSY) measurements were performed using Bruker Avance 400 MHz spectrometer equipped with a Great 1/10 pulsed gradient unit and a direct probe at 297 K. A LED[3] pulse sequence (ledbpgp2s) was used for the diffusion experiments with a sine shape pulsed gradient duration δ(P30) of 1.0 ms incremented from 0.68 to 32.4 G cm^{-1} in sixteen steps. The pulsed gradient separation Δ(D20) was 75 ms, the spoil gradient (P19) was set to 600 μs, and the eddy current delay (D21) was 5 ms. The reported diffusion coefficients were obtained using the T1/T2 relaxation module in TopSpin 2.1 software. DOSY measurements were performed in $CDCl_3$ for the resorcinarenes **1** and **2** and their 1:1 mixtures with bivalent linkers **A**-**C**. Literature value of diffusion coefficient for $CHCl_3$ is 2.332×10^{-9} m^2s^{-1} in 298 K.[4] The average values of the determined diffusion coefficients (*D*) are presented in table S1.

Table S2. Average diffusion coefficients *D* (m^2s^{-1}) of resorcinarenes **1** and **2** and their 1:1 mixtures with linkers **A**-**C** at 297 K**.**

Sample	***D*** **(m^2s^{-1})**	***D*****$_{solvent}$** **(m^2s^{-1})**
1	5.93×10^{-10}	-[a]
1·A	5.97×10^{-10}	-[a]
1·B	6.01×10^{-10}	-[a]
1·C	6.08×10^{-10}	2.30×10^{-9}
2	5.94×10^{-10}	2.78×10^{-9}
2·A	5.85×10^{-10}	2.57×10^{-9}
2·B	5.82×10^{-10}	2.05×10^{-9}
2·C	5.82×10^{-10}	2.18×10^{-9}

[a] Diffusion coefficient could not be determined because $CDCl_3$ signal overlapped with another signal.

[3] S. J. Gibbs and C. S. Johnson Jr., *J. Magn. Reson.* **1991**, *93*, 395-402.
[4] H. Kato, T. Saito, M. Nabeshima, K. Shimada and S. Kinugasa, *J. Magn. Reson.* **2006**, *180*, 266-273.

5. Computational Studies

Table S3. Calculated relative signal shifts of fluorine atoms of linkers **A** and **B** in ^{19}F NMR.

	Interaction	**Δppm**
linker **A**		0
	···$HCCl_3$	+1.13
	···2 $HCCl_3$	+2.09
	···4 $HCCl_3$	+3.61
	avg ···$HCCl_3$	*+2.28*
	single XB (···N)	+2.07
	double XB (···N)	+3.63
linker **B**		0
	···$HCCl_3$	+1.00
	···2 $HCCl_3$	+2.02
	···4 $HCCl_3$	+3.95
	avg ···$HCCl_3$	*+2.32*
	single XB (···N)	+3.38
	double XB (···N)	+6.66

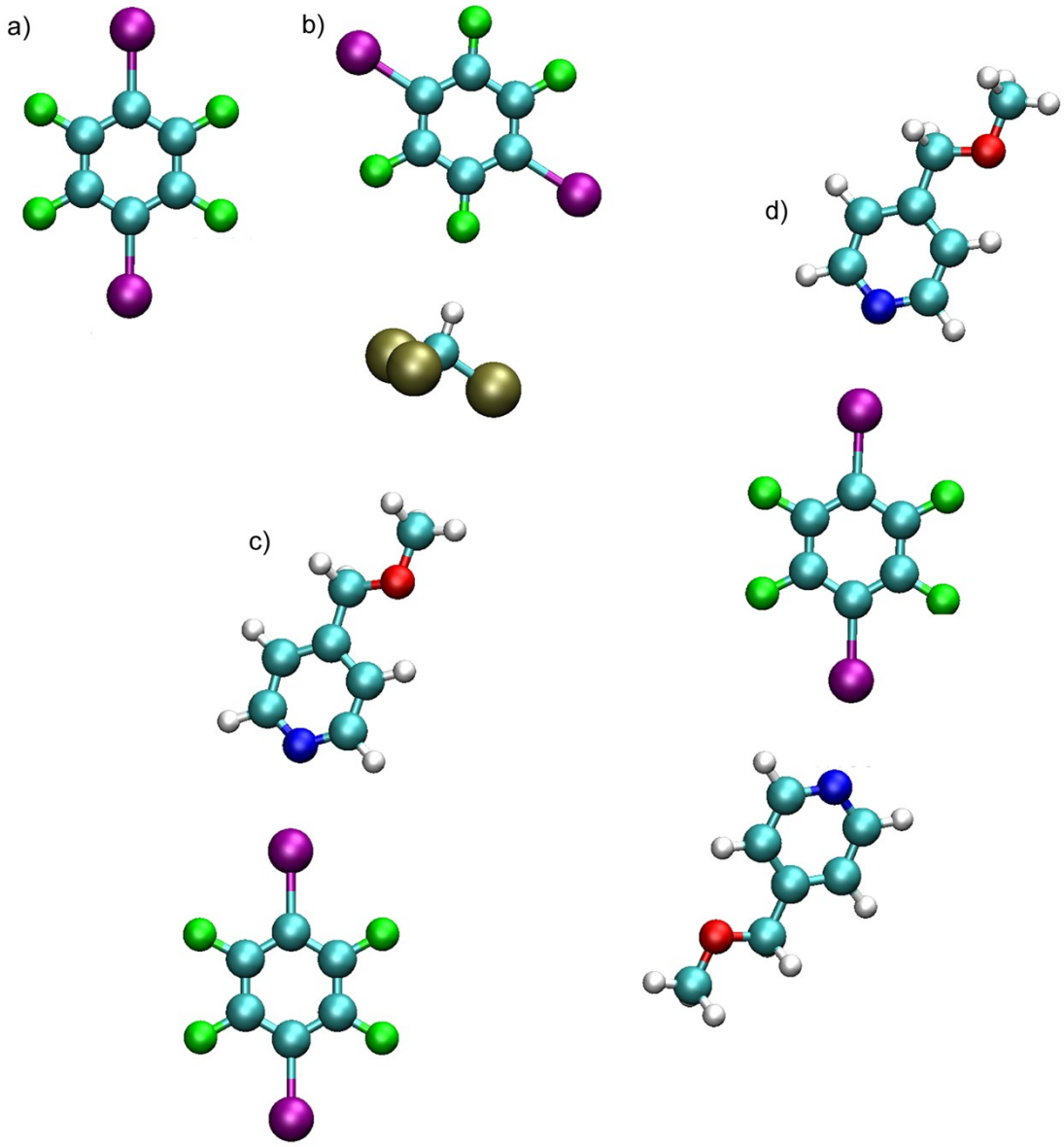

Fig. S24 Models systems of resorcinarene **2** and iodo-linker **B** used in the DFT calculations, (a) L, (b) L···$HCCl_3$, (c) L···R and (d) L···R···L.